Historical review of seismic studies on structure of Volcanoes (*)

R. Piermattei - W. M. Adams (**)

Received on June 20th, 1973

Riassunto. — Metodi sismici di investigazione in zone vulcaniche possono essere considerati di tipo attivo, in cui la sorgente di energia è controllata dall'investigatore (esplosioni), o passivo, in cui la sorgente di energia è naturale (scosse sismiche). Questo lavoro intende dare un quadro delle ricerche più significative che sono state fatte in Giappone, Unione Sovietica, Stati Uniti e altrove.

Summary. — Seismic studies of volcanic areas can be considered either active, in which the source is controlled by the investigator, or passive, in which the natural sources are used. This paper reviews some of the more significant work that has been done in Japan, Russia, the United States, and elsewhere.

Introduction

Volcanoes and volcanological phenomena have been studied for many years using petrology, mineralogy, seismology, and other disciplines of geology and geophysics. Direct exploration of the Earth beneath active volcanoes is not yet feasible, hence, generalizations made on the mechanism of eruption and internal structure have had to be mostly of a qualitative or speculative nature. It is only in the past decade that quantitative studies on the structure of volcanoes and the mechanics of volcanic phenomena have started to appear in the literature, and the bulk of them have appeared in the past three or four

(*) Hawaii Institute of Geophysics Contribution No. 596.

(**) Hawaii Institute of Geophysics, University of Hawaii, Honolulu 96822 (U.S.A.)

years. Most of the knowledge acquired during this "great leap forward" was obtained from seismic data recorded partly by standard permanent stations but mostly by temporary stations equipped with high-frequency, high-gain instruments.

In the study of volcanoes we are faced with the situation that the geophysicist usually encounters in most of his work, namely, he has a set of data observed on the surface and caused by phenomena occurring at depth. The approach is then basically one of constructing models to fit the observations and this usually leads to a non-unique solution. The use of all the tools of geophysics is required to reduce the number of acceptable models to a minimum.

Seismic studies of volcanic areas can be grouped into two categories: (1) active seismic experiments, i.e., refraction and reflection surveys; and (2) passive seismic experiments, i.e., analysis of earthquake or microearthquake data from permanent or temporary stations. We will review the recent literature to obtain a general picture of the progress made so far.

Active Seismic Experiments (Refraction and Reflection Surveys)

For several reasons, refraction and reflection seismology have not been employed very frequently in volcano studies. The most important of these reasons are: (1) the heretofore lack of economic motivation — which now exists in relation to the new importance assumed by volcanoes as possible sources of thermal energy; (2) the high attenuation of seismic energy by the highly fractured and porous volcanic materials and loose deposits, such as ash and pyroclastic deposits; (3) the high noise levels; and (4) the logistic difficulties due to the ruggedness of volcanic terrain.

Japan — The few attempts that have been made to use active methods have met with varying degrees of success in Japan. Some of the earliest seismic surveys on volcanoes were carried out on Showa Shinzan [16] and on Aso volcano [32].

Hawaii — Several seismic surveys have been carried out in the Hawaiian Islands. One, using refraction traverses, both on land and offshore, resulted in a structural model (shown in Figure 1) of the Koolau volcanic range [10], which is the youngest of the two major ranges comprising most of the island of Oahu. The instrumentation

used in this study consisted of HS 4.5 cps geophones, Fortune Electronics model T-1 transistorized amplifiers, and SIE oscillographic cameras. One of the interesting discoveries of this study was the presence of high velocity, 7.6-7.7 km/sec, material at shallow depth, 5 to

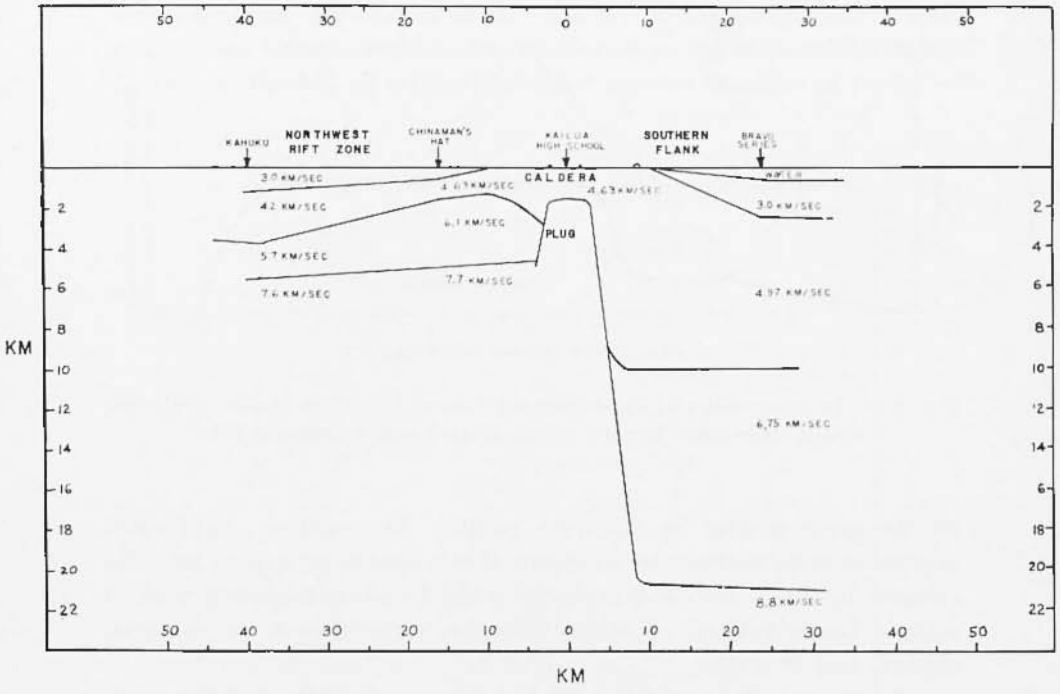

Fig. 1. – A structural cross section of Koolau Volcano on the island of Oahu, Hawaiian Islands [from Furumoto et al. ([10])].

6 km under the rift zone, and in the plug of the volcano at about 2 km depth. During the course of the same study, the dimensions and the depth of the high-velocity plug underlying the caldera were obtained from refraction data; the possible presence of a magma chamber (shown in Figure 2) at a depth of between 3 and 4 km was inferred from reflection arrivals ([2]).

The island of Hawaii, the only island of the Hawaiian Islands chain with active volcanoes, was the site of a refraction survey carried out with the same instrumentation used in the previously mentioned Koolau survey ([11]). This survey, carried out on a cinder cone at an

elevation of over 13,000 feet on the top of Manna Kea volcano, was the first on the internal structure of a cinder cone. It failed to show the presence of a hidden lava plug or any solid layers. The interpretation of the travel-time data used the method of aplanatic surfaces ([12]) because conventional interpretation techniques could not be used due

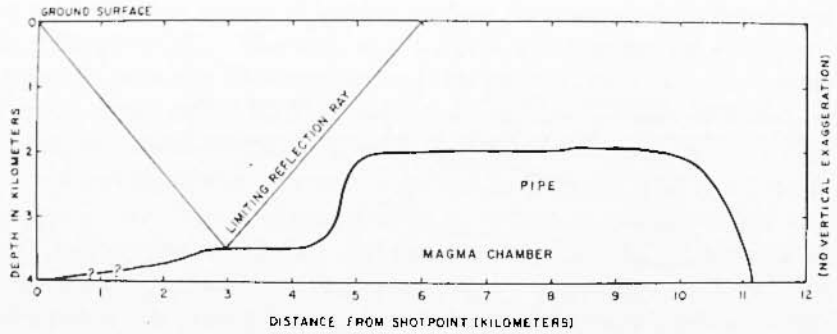

Fig. 2. — Interpretation of the refraction data obtained on Koolau Volcano, Oahu, Hawaiian Islands [from Adams and Furumoto ([2])].

to the great scatter in the data points. This method, previously applied only to outline the structure of salt domes, proved to be quite efficient in this study, and probably could be advantageously used in seismic investigations of other volcanic features such as calderas, craters, and so forth.

Ryall and Bennett ([27]) published the results of a 115-km long, partly reversed, refraction profile carried out in 1963 on Hawaii, from Hilo on the eastern seaboard, across Kilauea volcano, to Kalae on the southern seaboard (see Figure 3). Radial arrays of six vertical 2 cps seismometers spaced 0.5 km apart received the signal produced by explosions of charges ranging in size from 48 up to 250 pounds of nitro-carbo-nitrate detonated offshore at two positions, at each end of the profile. One additional 100-pound charge was detonated on land near the Hawaii Volcano National Park to obtain additional data for the portion of the profile covering the summit of Kilauea. The recording was accomplished photographically by a low-frequency refraction system (VLF-1, Texas Instruments). Additional data were provided by the Hawaii Volcano Observatory Kilauea network, whose stations use short-period 1 cps seismometers and peak magnifications of 20,000 to 40,000 at 0.2 sec, and by a system, consisting of matched short-

period seismometers, amplifiers, and a multichannel photographic recording oscillograph, used by a team of visiting Japanese scientists.

The composite travel time curves shown in Figure 4a, consisting of the Hilo and Kalae profiles plotted together, show evidence of the difficulties encountered in the interpretation due to the following reasons: (1) the *Pn* branch of the Hilo profile has two breaks in slope rather than being a straight line and overlaps the Kalae line for only 25 km; (2) the lack of reversal for the other two branches of the travel

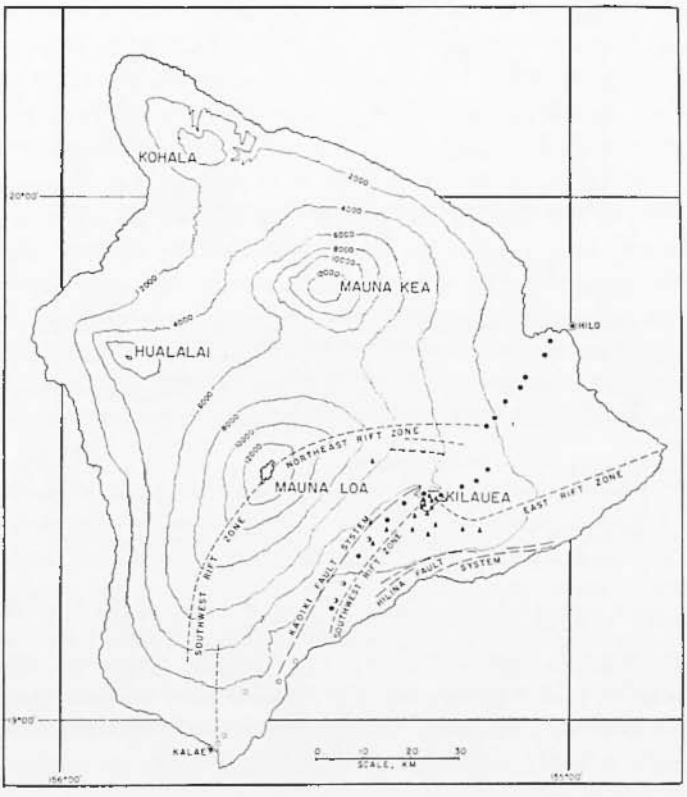

Fig. 3. – A topographic map of the island of Hawaii in the Hawaiian Islands. Elevations are in feet. Rift zones are denoted by short-dashed lines; fault systems, by long-dashed lines. Circled dots show location of the shotpoints; solid triangles show locations of the fixed stations. Solid dots are temporary stations for the Hilo shots; open circles are temporary stations for the Kalae shots. Circles that are half-closed show locations of temporary stations used for both shot series [from Ryall and Bennet ([27])].

time curves; and (3) the gross disparity between the apparent velocity and the intercept time of the intermediate branches. Due to these difficulties, seismic velocities for the various layers had to be assumed and the interpretation of the travel-time data had to be carried out by approximations based on these initially assumed values. From all the acceptable structural models obtained in this manner, an aver-

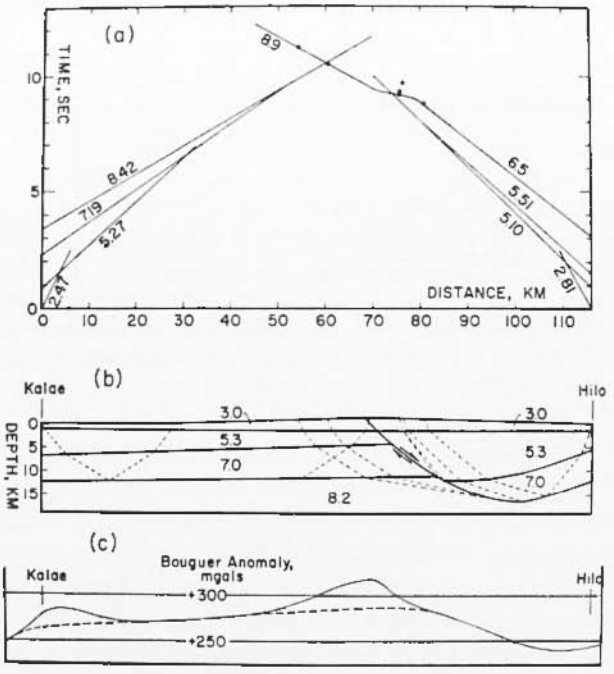

Fig. 4 – (a) Travel-time curves deduced from the Hilo-Kalae data. (b) Model of crustal structure along the Hilo-Kalae profile, as deduced from the data with restricting assumptions. (c) Bouguer anomaly along the Hilo-Kalae profile, as taken from Kinoshita et al. ([20]). The dashed lines are the Bouguer anomaly adjusted for assumed shallow high-density material [from Ryall and Bennet ([27])].

age crustal structure consisting of three layers was obtained (see Figure 4b). This model shows the presence of a normal fault with a total vertical offset across it of 7.5 km. This fault could be related to either the northeast rift of Mauna Loa or the east rift of Kilauea or both (see Figure 3) through observations made at two of the fixed stations

of the Hawaiian Volcano Observatory at which a delay of the arrivals was observed — as expected if the fault crosses the refraction line in a northwesterly direction.

The interpretation of Ryall and Bennett seems to receive support from the gravity profile shown in Figure 4c after removal of the two highs above the dashed portion of the line, if these highs are assumed to be due to near-surface zones of dense material — a shallow magma chamber under the summit of Kilauea and dense material at the southwest rift zone of Mauna Loa.

Additional seismic refraction surveys along the northeast, southwest, and west coasts of Hawaii, carried out in 1964 by U. S. Geological Survey, were reported by Hill ([17]). Five refraction units, each consisting of six vertical seismometers (1 cps) in a linear array 2.5 km long, both magnetic and photographic multi-channel recorders, were placed at 25 km intervals along each coast to monitor shots consisting of 300 to 400 pounds of nitramon fired offshore at 10-km intervals.

Additional recordings were provided by the fixed stations of the Hawaiian Volcano Observatory network, which also recorded the data from three 500-ton chemical charges detonated by the U. S. Navy in 1965 on the island of Kahoolawe as part of the Sailor Hat program. The latter were also recorded by two mobile units. Figure 5 gives the location of stations and shotpoints as well as the location of two seismic refraction profiles shot by Scripps Institution of Oceanography in 1962.

From this work the crustal structure was found to be composed of an uppermost layer formed by the accumulation of lava 4 to 8 km thick, with P velocities increasing within it from 1.8 to 3.3 km/sec. This layer overlies what is probably the original oceanic crust, also having a thickness ranging between 1 and 8 km, with P velocities of 7.0-7.2 km/sec which in turn overlies the upper mantle with a P velocity of 8.2 km/sec under most of the island and 8.1 km/sec under Kilauea. The structure under the northeast and southwest flank of Kilauea is also composed of two layers, of which the upper has P velocities ranging from 1.8 to 5.1 km/sec, and the lower, 7.1 km/sec. Their combined thickness is 11 to 12 km. Figure 6 shows an idealized crustal structure of a Hawaiian volcano, based on Kilauea mostly. The structure under the central part of the volcano is perforce largely hypothetical, and more data are needed.

ALASKA — Lamont Geological Observatory's seismological program in Alaska's Katmai Peninsula included refraction traverses in

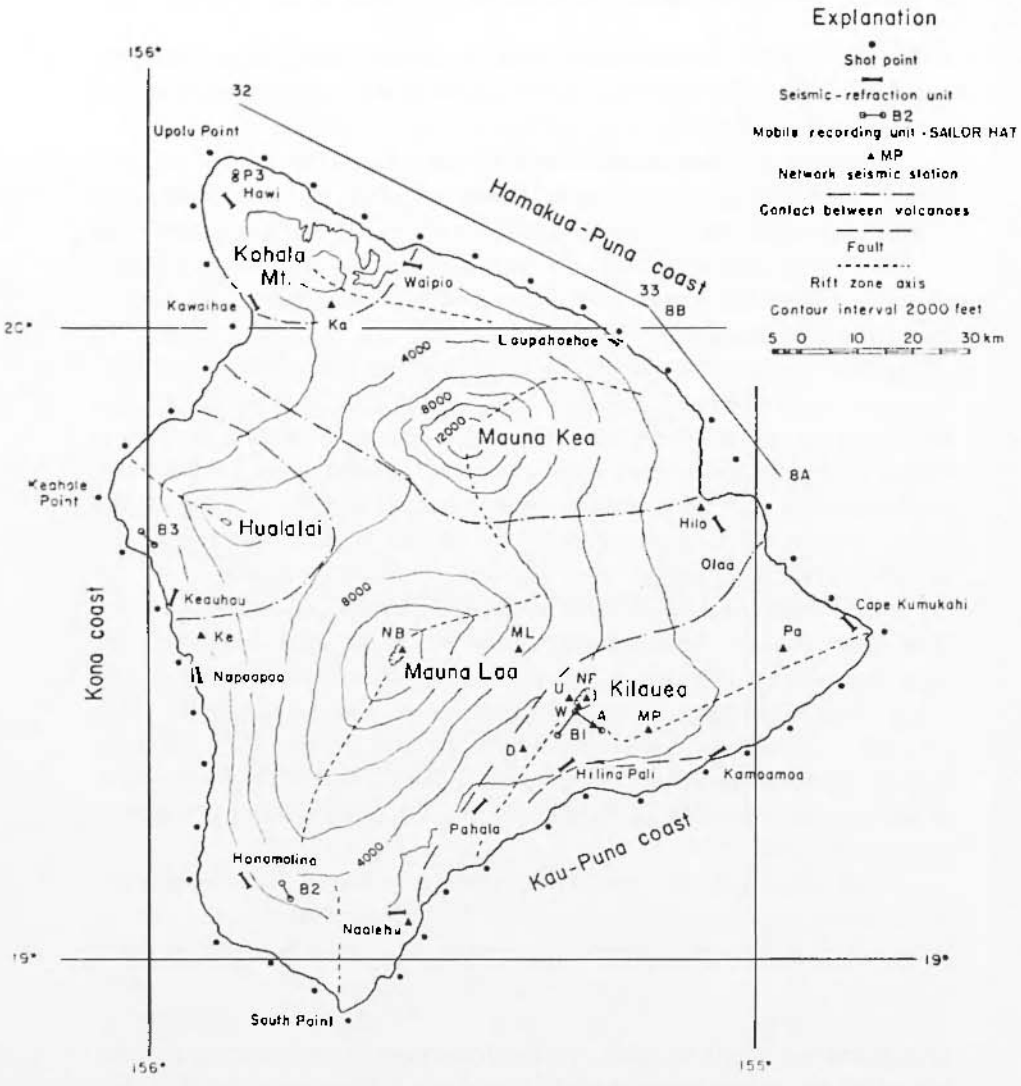

Fig. 5 – Topographic map of Hawaii in the Hawaiian Islands. Elevations are in feet. Locations of shotpoints, mobile recording units, and permanent seismograph stations are shown, as defined in the legend. Lines 32-33 and 8A-8B are approximate locations of the seismic-refraction profiles shot by Scripps Institution of Oceanography in 1962. Major rift zones are indicated by short dashed lines. The lines of alternating dots and dashes separate the five volcanoes according to surface geology.

Abbreviations for seismograph station locations are:

A, Ahua; **D**, Desert; **Ka**, Kamuela; **Ke**, Kealakekua; **ML**, Mauna Loa; **MP**, Makaopuhi; **NB**, North Bay; **NP**, North Pit; **Pa**, Pahoa; **U**, Uwekahuna; **W**, West Pit [from Hill [17]].

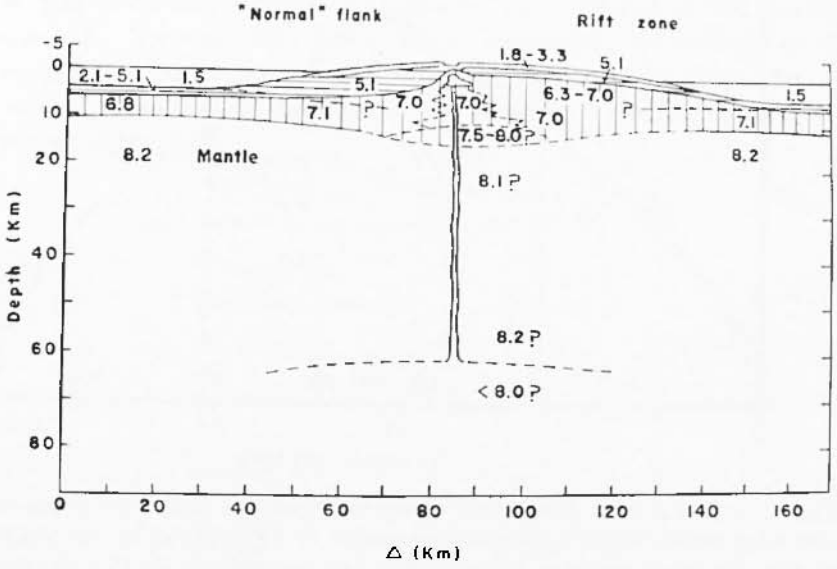

Fig. 6. – Cross-section of a typical Hawaiian volcano (based largely on data from Kilauea). Dashed lines indicate less definite boundaries between *P*-wave velocities, given in km/sec. The section to the right of the vent shows the structure under a major rift zone; the section to the left, the structure under a typical flank. The structure under the summit represents the shallow magma chamber and main conduit of the volcano suggested by Eaton and Murata [5] and a possible configuration of the cumulate-filled fossil magma chamber suggested by Jackson [18]. The decrease in *P*-wave velocity suggested at 60 km is hypothetical [from Hill [17]].

the Katmai National Monument. The instrumentation for the traverse reported by Ward and Matumoto [30], whose interpretation is shown in Figure 7, consisted of a Lamont short-period amplifier, a chart recorder with 5 mm/sec speed, and a geophone with 4.5 cps natural frequency. Three more refraction traverses (see interpretation in Figure 8) were carried out by Sbar and Matumoto [28] using four HS-1 4.5 cps geophones, a S. I. E. Model GTR-200 four-channel amplifier, and a Century 666 six-channel oscillograph using direct writing paper. The locations of these profiles are shown in Figure 9.

Even though due to National Parks regulations explosives could not be used and the only energy source was a 10-pound sledge hammer striking an aluminum wedge, these traverses provided information on the thickness and extent of the 1912 pyroclastic deposits in the Valley

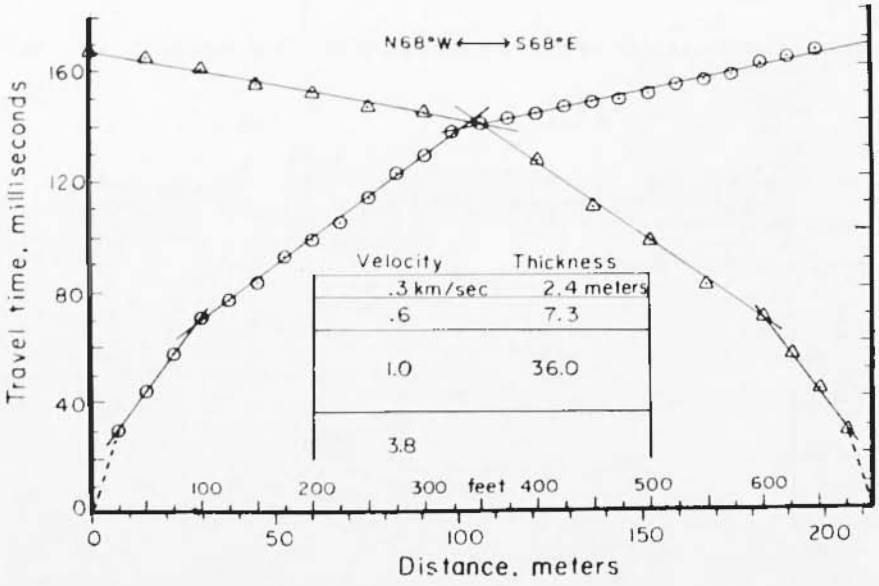

Fig. 7. – Travel-time data, fitted curves, and deduced model for a seismic refraction profile about 1.6 km east-southeast of Three Forks in the Valley of Ten Thousand Smokes. The dashed line corresponds to the assumed surface layer [from Ward and Matumoto (30)].

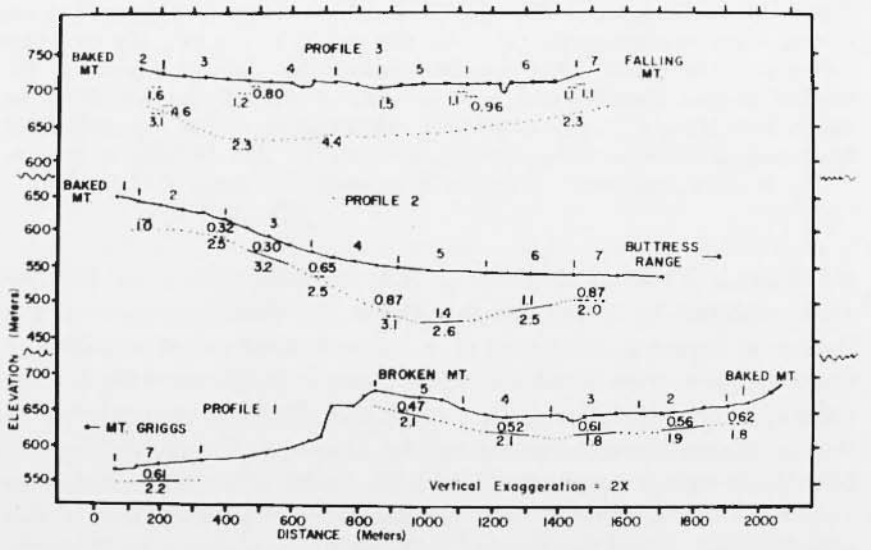

Fig. 8. – Three refraction profiles taken in the Valley of Ten Thousand Smokes, Katmai, Alaska. Vertical exaggeration of 2; velocities in km/sec. Solid line indicates a reversed measurement; dashed line, an unreversed measurement. The dotted line is the assumed structure. The surface is denoted by a solid line. The points on the surface line are measured topography from Kienle (19) [from Sbar and Matumoto (28)].

of Ten Thousand Smokes and revealed the presence of moraines in the tuff. Two or three layers found, depending on location in the main body were interpreted as different phases or eruption; the increasing thickness of the deposit near Novarupta suggested it as the center of eruption.

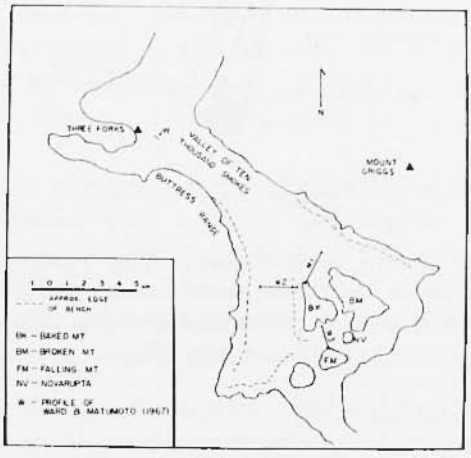

Fig. 9 – Map of the Valley of Ten Thousand Smokes, Katmai, Alaska, showing the location of the seismic refraction profiles of Ward and Matumoto ([30]), denoted by W, and of Sbar and Matumoto (1972), denoted by =||=1, =||=2, =||=3. The broken lines indicate topographic benches seen along the slopes of the surrounding ranges [from Sbar and Matumoto ([28])].

KAMCHATKA — A seismic refraction survey in a very active volcanic area is the one reported by Balesta and Farberov ([3]) of Piip Crater on the flank of the Kliuchevskoi Volcano in Kamchatka. Those authors were able to determine the structure and the size of the injection area of magma in the upper part of the conduit feeding the crater. Figures 10, 11, and 12 show the locations of the profiles and interpretations of the data. This is a first step towards understanding the mechanism of the formation of adventive craters on this volcano.

In their study, Balesta and Farberov carried out measurements of the velocity of seismic waves through fluid lava in the area of magma injection. Their observed *P*-velocities, ranging between 750 and 850 m/sec, seem low compared to laboratory studies.

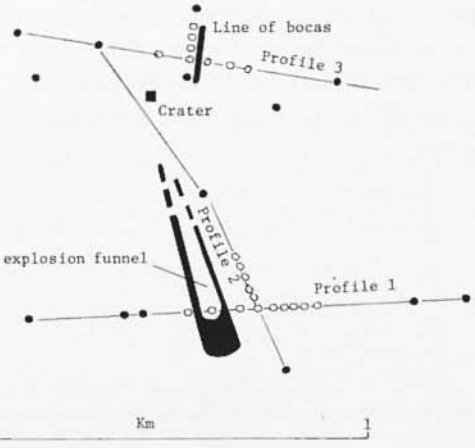

Fig. 10. – Map of seismic profiles around Piip volcano in Kamchatka. Solid points indicate the shotpoints; hollow circles, the location of the instruments; and solid lines, the profile arrangements [redrawn after Balesta and Farberov (3)].

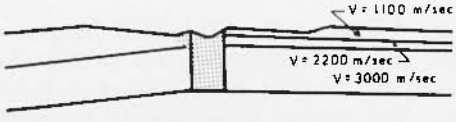

Fig. 11. – Model for seismic section along the lower profile, =|– 1, of Figure 10. The break-through fracture is at the center [redrawn after Balesta and Farberov (3)].

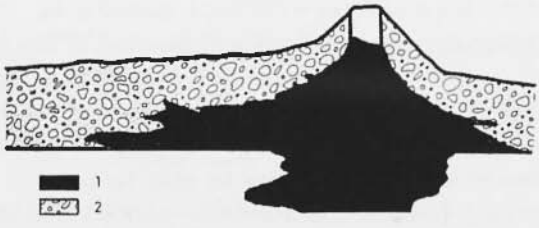

Fig. 12. – Schematic section across the break-through fracture of Piip volcano. The central material (1) is injected lava, surrounded on both sides by pyroclastic material (2) [redrawn after Balesta and Farberov (3)].

Passive Seismic Experiments

Since the work of Omori and others in the 19th century, the study of earthquakes from volcanic areas has proved valuable in providing information on the internal structure of volcanoes. Depending on the amount and quality of the available data, two major directions of investigation can be considered; these are (A) seismicity studies, and (B) studies to determine the presence and size of zones of melting below the surface by analysing the attenuation of seismic body waves travelling through them, or the screening effect of such zones on the shear waves.

Although the first reports on the attenuation of seismic waves by molten magma bodies were based on seismograms obtained from standard seismograph stations, most of the work in recent years used portable microearthquake recording-systems. The latter have the advantage of supplying a great amount of data in a short period of time, and in areas far from standard seismograph stations.

Kamchatka — Portable stations used in conjunction with conventional seismic stations gave good results in locating magma chambers under some of the Kamchatka volcanoes, considering the shortcomings of standard stations, i.e. the constraint of the wave paths (over which there is no control), the scarcity of stations at suitable locations, and the fact that standard seismographs have too low a frequency response to detect the shadow caused by magma chambers less than a few kilometers in diameter.

The first observational work on locating magma chambers was reported by Gorshkov [13]. He estimated the depth of the magma reservoir below the Kliuchevskaya volcanic group at a depth of 50 to 70 km, based on the attenuation of *S* waves from distant earthquakes. After these promising results, the study of the attenuation of transverse seismic waves under the Kamchatka volcanoes was intensified. Fedotov and Farberov [8], using seismograms from five stations, discovered the presence of a zone where *S* waves are screened at a depth of 20 to 80 km under the Avachinskaya group of Kamchatka volcanoes. The diameter of this zone is about 25 km and the absorption of *S* waves there is four times higher than that for the entire region, i.e., 0.039 ± 0.012 km^{-1} at 1 to 2.5 Hz.

Other zones of low viscosity at 30 to 140 km depth where high attenuation of *S* waves occurs, interpreted as magma chambers, have

been reported by Gorshkov [14] to have been identified below certain volcanoes of eastern Kamchatka and in the Kliuchevskaya group, as a result of the work of Farberov and Gorelchik [6] and that of Firstov and Shirokov [9]. The latter authors investigated the screening of both P and S waves from intermediate focus events near the Kliuchevskaya volcanic region. The anomalous zones where the seismic energy of both P and S waves is scattered and attenuated lie at depths of 35 to 110 km. The method of analysis used in this study involves the use of seismograms from two stations whose locations are such that the paths of the seismic waves from the foci of the events considered penetrate the chamber volume for one station and lie outside it for the other station, as shown in Figure 13. The ratios of amplitudes at the two stations are calculated for both P and S waves for all events considered; after reduction to a single hypocentral distance and correction for conditions at the stations they should be close to 1.0 if the attenuation characteristics along the two paths are similar, since the other factor that could possibly affect these ratio, — the effect of focal mechanism — could be neglected because of a solid angle of less than 20° from focus to stations. The value of the amplitude ratios was found to deviate considerably from 1.0 for deep earthquakes, and the ratios of periods at the two stations for both P and S waves corresponding to maximum amplitudes were also found to be greater than expected, indicating that the station for which the wave paths pass through the volcanic region records greater periods for anomalous events.

The values of amplitude and period ratios indicate the presence of anomalous features acting as obstacles along the path of the waves, possibly magma chambers which scatter and absorb the seismic energy. For first arrivals of about 5-km wavelength, it can be assumed that the wave front propagates along the shortest time path. P and S velocities are practically constant between 35 and 200 km depth in the Kamchatka region, and a seismic ray is therefore a straight line and can be determined by azimuth and angle of incidence on the Mohorovicic discontinuity.

A plot of the anomalous earthquakes in terms of these angles defines the areas of possible melting, shown in Figure 14, as projected on the Earth's surface. These zones are concentrated at depths of 35 to 40 km, 40 to 45 km, and 110 km with portions reaching 60 to 80 km and are entirely aseismic as would be expected if they represent pockets of low viscosity material. A different approach was used by Farbe-

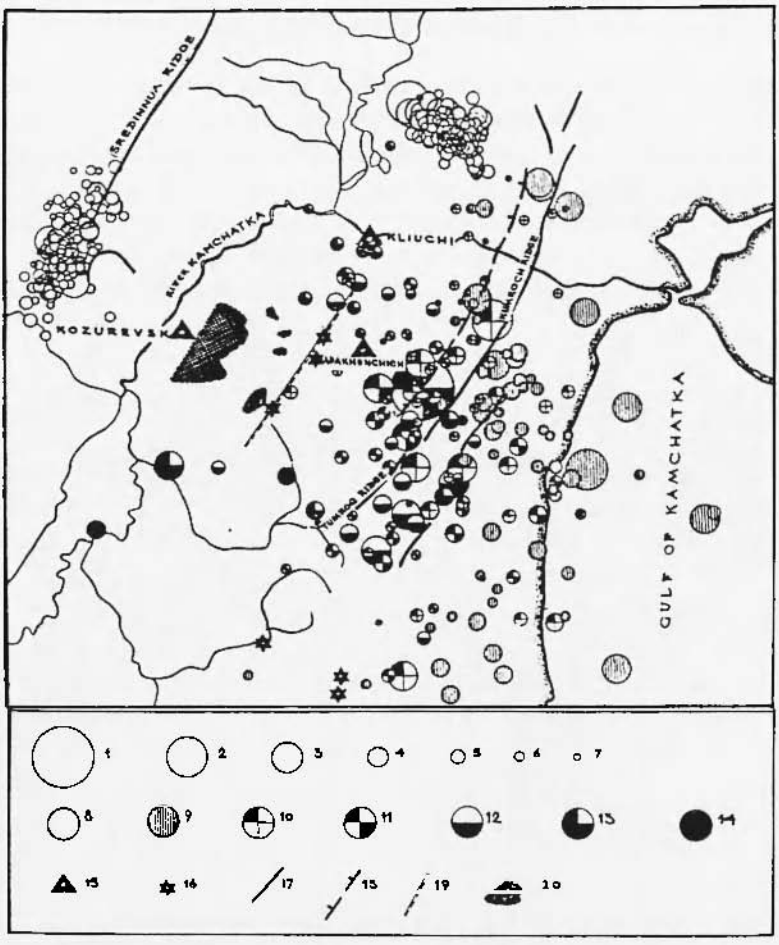

Fig. 13. – Map of the epicenters of deep-focus earthquakes in the vicinity of the Kliuchevskaya group of volcanoes, Kamchatka, for the time interval 1964 to 1968 [from Firstov and Shirokov ([8])].

The diameter of the open circles is proportional to the energy of the earthquake. Specifically, define K = log energy (joules), then,

Circle	1	2	3	4	5	6	7
K	13	12	11	10	9	8	7

The depth of the focus is coded in the interior of the circle.

Symbol	8	9	10	11	12	13	14
Depth (km)	0-20	76-100	101-125	126-150	151-175	176-200	more than 200

and the other symbols:

15	seismic stations
16	active volcanoes
17	ridges
18	the main tectonic fractures
19	line through the active volcanoes
20	projection of anomalous zones on the surface

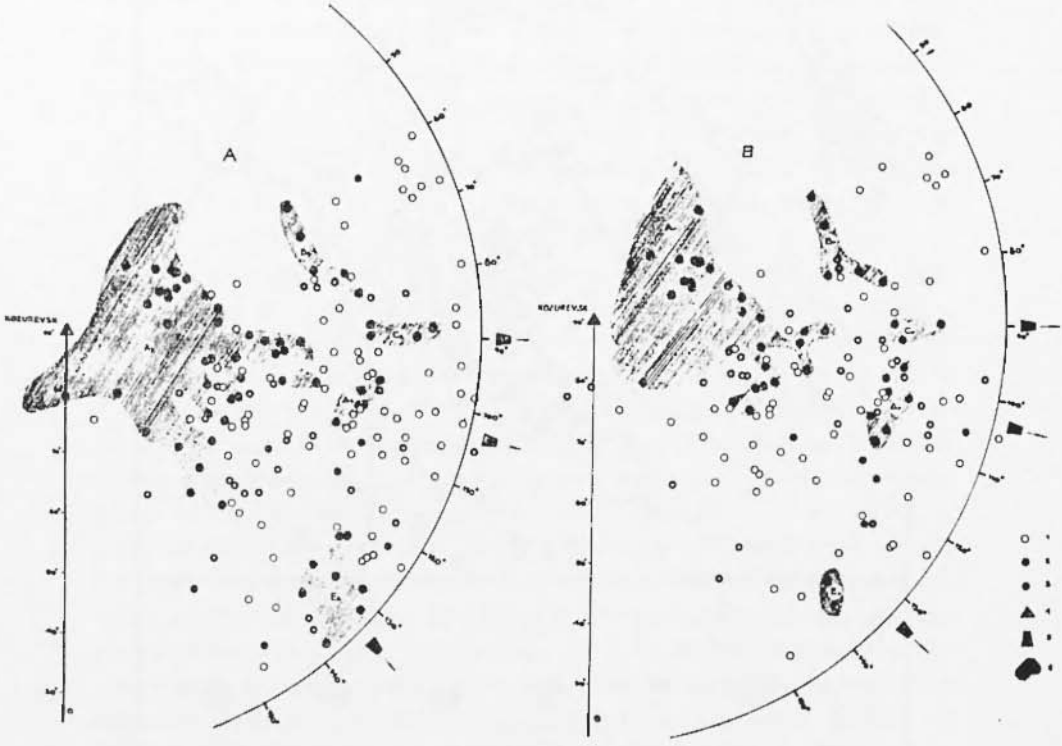

Fig. 14. – Projection of the earthquake rays on the unit sphere about Kozurevsk station in Kamchatka. Projection (A) is for S-waves; projection (B) for P-waves. The meaning of the symbols is obtained by defining K as the amplitude ratio of the respective wave at any station to the same wave observed at Kozurevsk [from Firstov and Shirokov [9]].

Then, following, the legend,

Symbol	*Meaning*
Open circle	Normal depth earthquakes with K more than 0.66.
Small filled circle	Intermediate depth earthquakes with K between 0.42 and 0.66.
Large filled circle	Anomalous earthquakes with K less than 0.42.
Triangle	The station, Kozurevsk, to which the projection is made.
Truncated triangle	Azimuths to the active volcanoes.
Glob of solid spots	Zones of concentration of anomalous earthquakes.

rov and Gorelchik (6) to locate the zones of anomalous attenuation of seismic waves in the region of Avacha-Koryakskaya group of volcanoes. Those authors made use of seismograms from five stations whose instruments have a flat frequency response in the 1 to 5 Hz range and a magnification of 7,000 to 10,000. One of the stations was used as reference since the paths from the foci to the station lie outside the volcanic region. The parameter considered for analysis is the absolute

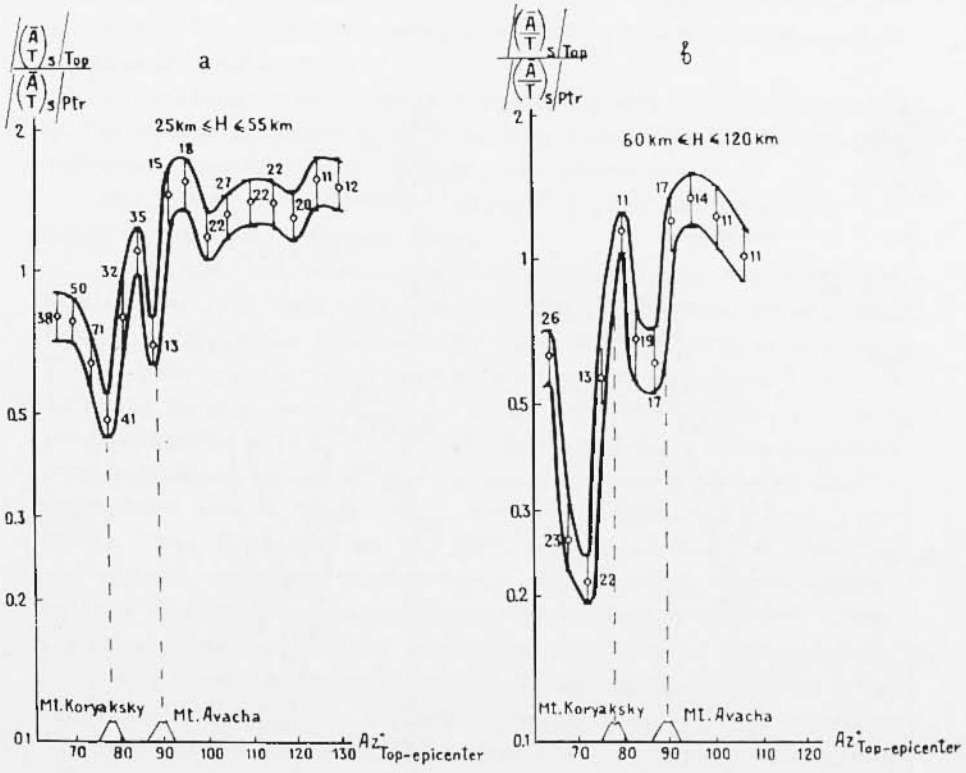

Fig. 15. – Denote the ratio of the amplitude to the period for the *SH* wave by $(A/T)_{SH}$. Then form the ratio of a pair of these ratios, the denominator being the reference station, Petropavlovsk. Depicted are diagrams of the ratio of ratios versus azimuths from the stations to the earthquake epicenters. On the left is the diagram for earthquakes having focal depth from 25 to 55 km; on the right, from 60 to 120 km. The means are plotted as open circles, with the number of data points written nearby. The 70% confidence limits have been included [from Farberov and Gorelchik (6)].

value of the maximum amplitude-to-period ratio of *SH* waves, as obtained from both horizontal components for each of the 400 events studied at each station. This ratio is then compared to the corresponding one for the reference station. All the other factors affecting the attenuation of the wave are corrected for in the same manner as described for the previously discussed work of Firstov and Shirokov (9).

The results of the analysis for one station are shown in Figure 15, where the events studied are divided into two groups on the basis of focal depth; and in Figure 16 for two more stations. The minima in

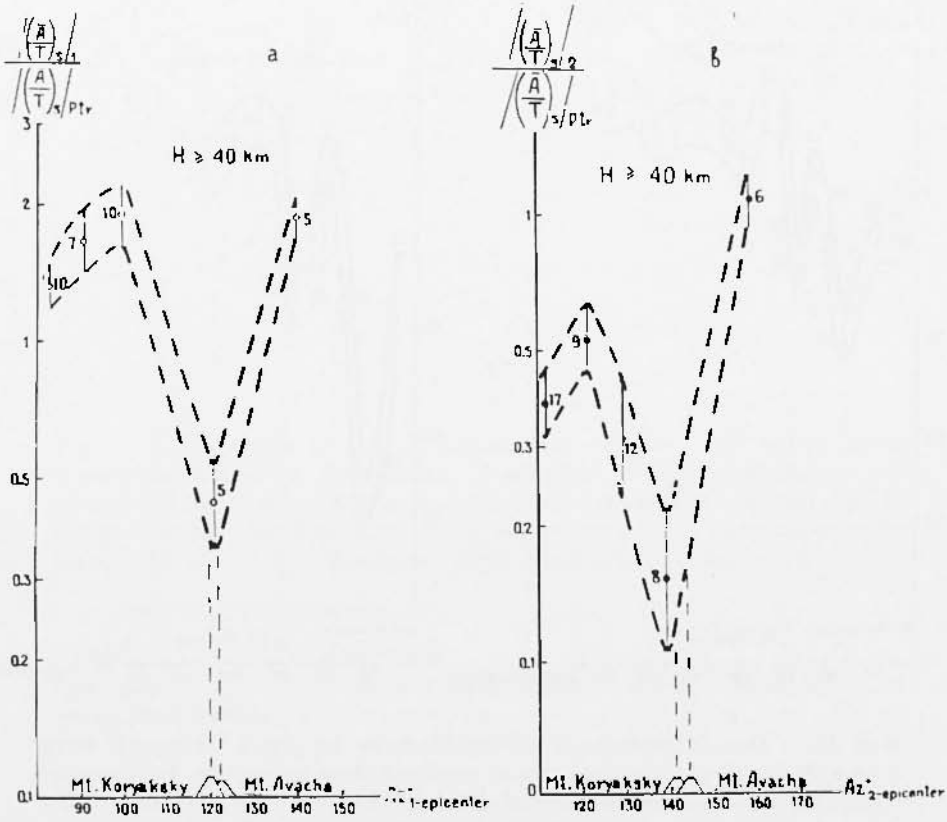

Fig. 16. – The notation is similar to that of Figure 15. On the left is the ratio of ratios versus azimuth from station to the epicenter for temporary station 1; on the right, for temporary station [from Farberov and Gorelchik (6)].

these curves correspond to the azimuths from the stations to the volcanoes. The parameters necessary for the determination of the minimum size of the obstacles causing the attenuation of the *SH* waves are the source-to-obstacle distance X_o, the obstacle-to-station distance X, and the ratio between the wavelength and the cross dimensions of the obstacle.

Minimum dimensions of the obstacles were calculated and found to be 8 to 30 km across, and their depth ranged between 30 and 100 km. A contour map is shown in Figure 17. The boundaries of the obstacles also delimit aseismic areas, as expected if these zones contain materials of viscosity low enough to prevent the build-up of stresses large enough to generate earthquakes.

The map shown in Figure 18 is a summary compiled by Fedotov (7) of the magmatic chambers discovered to date under the Kamchatka volcanoes by studying the attenuation of seismic waves.

References to many other Russian studies on the subject are listed in the works discussed above.

ALASKA — The effect of the anomalous zones on the period was also observed by Matumoto and Ward (23) for *P* waves whose paths intersect the Alaska volcanic belt. The only volcanic area in the U.S.A. where seismic wave attenuation studies have been aimed at detecting magma reservoirs is the Katmai Peninsula of Alaska. In a program started in 1965, four stations were established (4) and equipped with instrumentation capable of recording microearthquakes of Richter magnitudes down to ranges below zero and frequencies between 1 and 10 Hz. Two of the stations had three components and the other two had vertical component seismometers. The recording was accomplished by a chart recorder and slow-speed magnetic-tape recorder. Using a method based on *P* and *S* arrivals, a high value of Poisson's ratio of 0.3 was found for the upper mantle, indicating the possibility of the existence of low-rigidity material, possibly magma. This evidence was corroborated by negative Bouguer gravity anomaly values, also indicating the possible presence of low density material. A study on the location of magma chambers in the region, based on the screening of *S* waves, was reported by Kubota and Berg (21). A map with the stations and epicenters located by using a structural model for the region derived by Berg *et al.* (4) is shown in Figure 19. It was observed that the amplitude of the recorded *SV* waves was always very small compared to that of the *SH*, and the theory shows that this should indeed be the case, if the magma pockets are assumed to have the

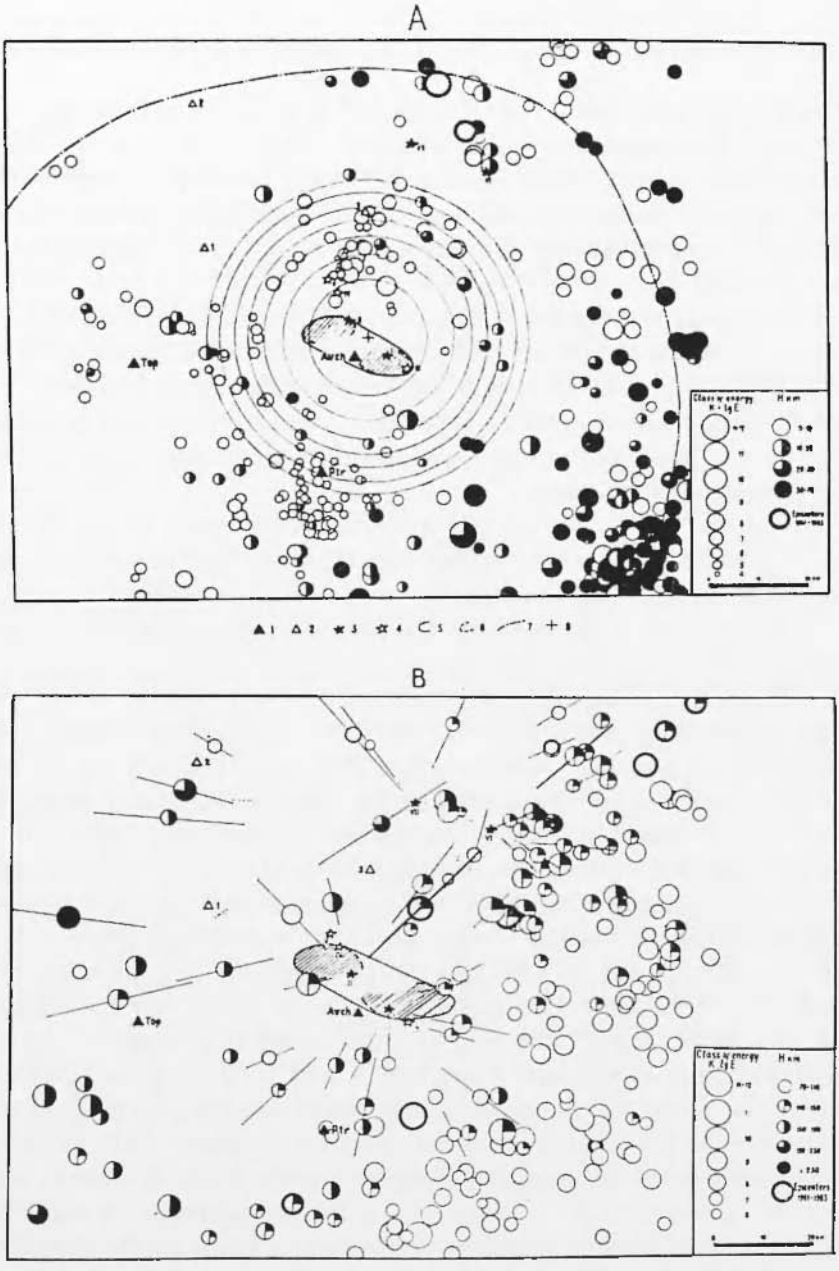

Fig. 17. – Two maps of earthquake epicenters in the Avacha Koryakskaya group of volcanoes, in Kamchatka, for 1961-1968. The upper map (A) is for those with normal focal depth (0 to 70 km); the lower, (B), for those with intermediate focal depth (70 to 250 km).
1. Stationary seismic stations, 2. Temporary seismic stations; 3. Active volcanoes: I, Mt. Avacha; II, Mt. Koryaksky; VI, Mt. Zhupanovsk; VII, Mt. Dzenzursky, 4. Extinct volcanoes: III. Mt. Kozelsky; IV, Mt. Aric; V, Mt. Aag. 5. and 6. Contours of the discovered seismic obstacle(s). 7. Limit of the area with earthquakes having energy greater than 10^6 joules. 8. The estimated center of the obstacles [from Farberov and Gorelchik (6)].

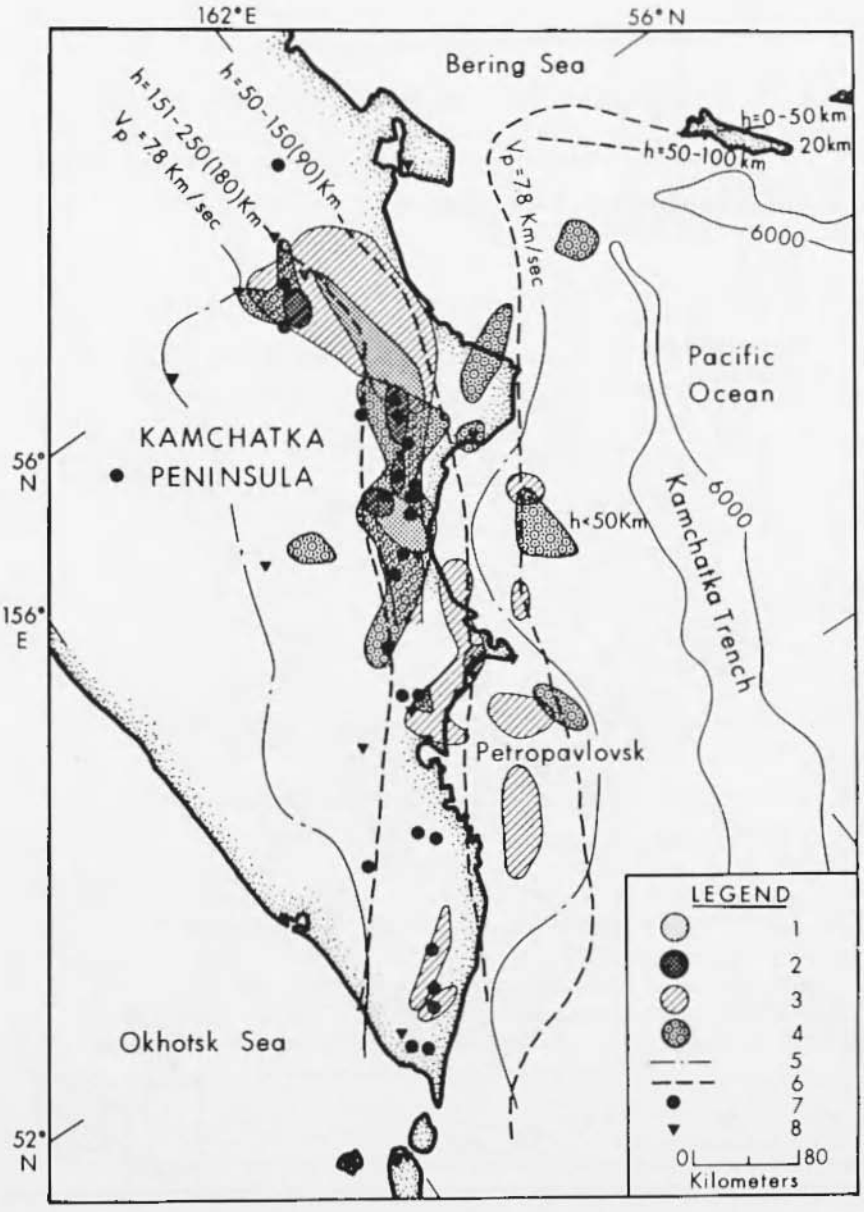

Fig. 18. – Map of the regions which screen P and S waves at depths of 30 to 100 km in the upper mantle beneath Kamchatka. Legend: (1) sites through which P waves pass poorly to three or more near stations; (2) sites for which S waves pass poorly to three or more near stations; (3) sites through which P waves pass poorly to two near stations; (4) sites through which S waves pass poorly to two near stations; (5) boundaries of the band within which longitudinal wave velocities V_p in the upper mantle layers are less than 7.8 km/sec; (6) isolines showing the mean position of earthquake foci having depths 0 to 50 km (nominally 20), or 50 to 150 km (nominally 90), or 150 to 250 km (nominally 180), as denoted on the respective isoline; (7) active volcanoes; (8) seismic stations. [Redrawn from Fedotov (?)].

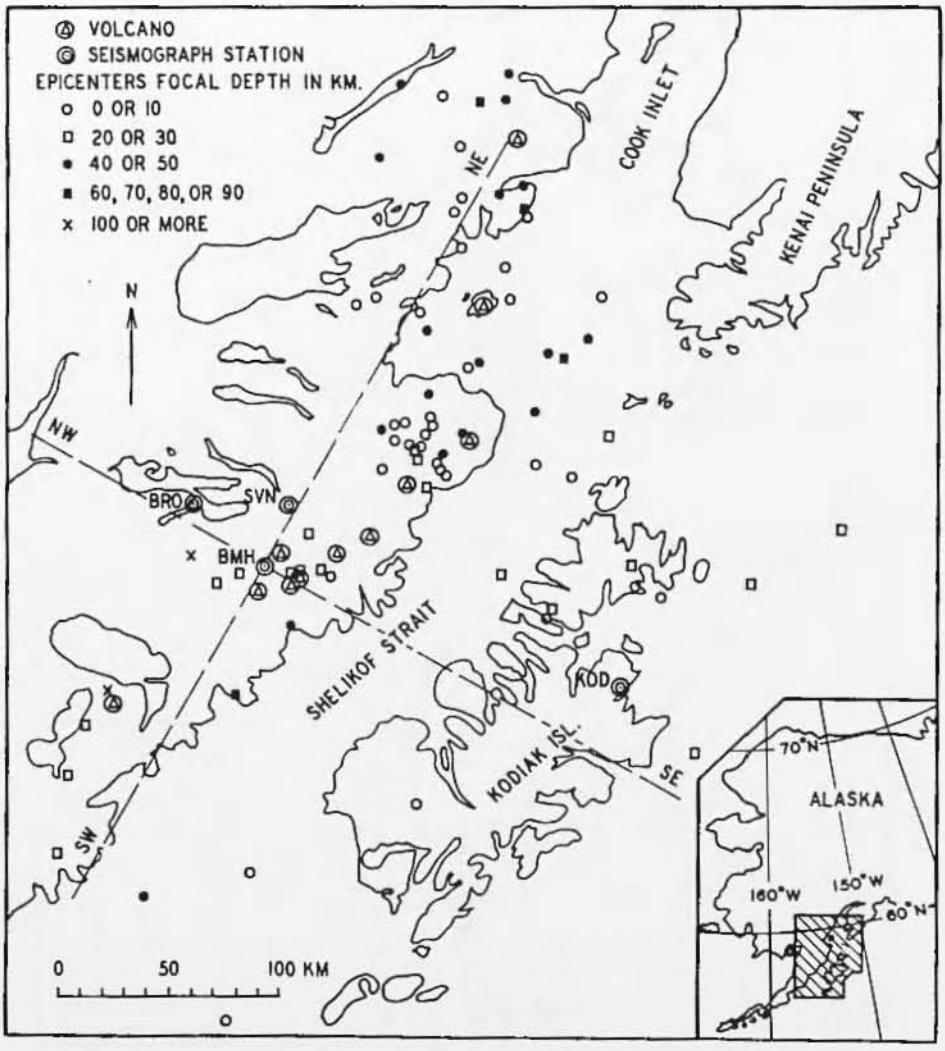

Fig. 19. – Map of epicenters located near Shelikof Strait, Alaska. See legend for meaning of symbols.
Seismic station abbreviation are: BMH, Baked Mountain; BRO, Brooks; KOD, Kodiak; SVN, Savonoski [from Berg *et al.* (4)].

shape of oblate spheroids. Figure 20 shows the behavior of the ratio of screening cross section for SH to that of SV waves (α) as a function of the ratio of the vertical to horizontal axis of a spheroid (ϱ) and a factor (μ) which is inversely proportional to the wavelength.

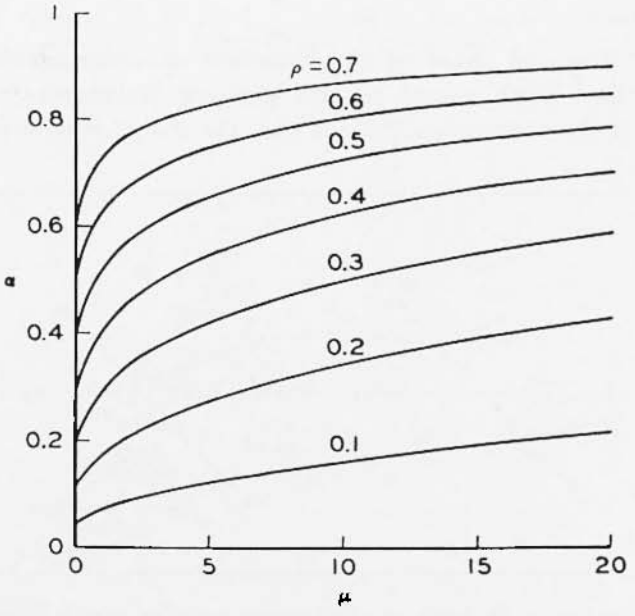

Fig. 20. – The ordinate is the ratio of the areas of shadow cross sections P_h/P_v; the abscissa is 2π times the ratio of the horizontal axis to the wavelength; and ϱ is the ratio of the vertical to the horizontal axis of the obstacle. To use this figure: enter on the horizontal axis at the appropriate value, proceed upward to the desired value of ϱ, and then left to the vertical axis to read off the ratio of screening cross-section of SH to that of SV. [from Kubota and Berg ([21])].

The absence of an S wave at a station only indicates that a magma chamber may be present somewhere along the ray path from the focus to the station. For two stations and two events, the lack of S waves can indicate either the presence of one magma chamber at the intersection between the two ray paths, or two separate magma chambers, as shown in Figure 21, hence the analysis consists in calculating as many wave paths as possible to all stations through the various layers of the crustal model for the region and mapping as many intersections as possible, thus minimizing the uncertainty inherent to the method. The

results of such an analysis are shown in Figure 22. The reliability of the method depends on the number of these intersections. The use of this method led to the identification of ten magma chambers shown in Figures 23 and 24.

The accuracy of the method is restricted by the factors discussed below:

(1) Size and shape of the chambers as compared to seismic wavelengths. With regard to this problem Matumoto ([22]) pointed out that, if the assumption is made that the size of magma chambers

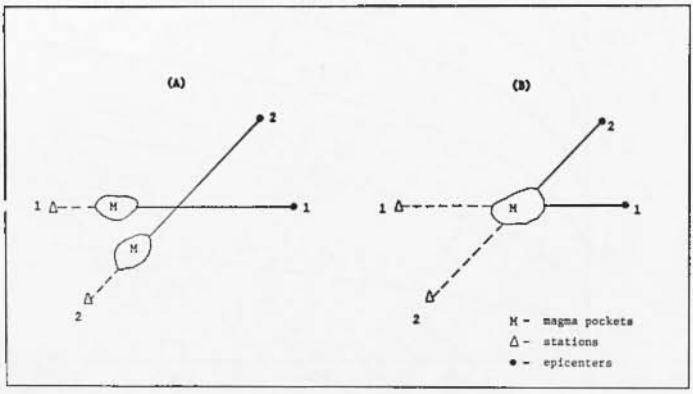

Fig. 21. – Diagram showing the ambiguity inherent in the interpretation of attenuated seismic waves. Either A or B can cause the same observational data. See Adams ([1]) for further details.

is comparable to that of calderas, and the values given by Williams and McBirney ([31]) for the average diameter of calderas of basaltic and silicious volcanoes are taken as representative, 6.8 and 13.9 km respectively, then most standard seismic-station short-period instruments such as the Benioff ($T_o = 1$ sec, $T_g = 0.2$ sec) have their peak response at frequencies so low that the normalized amplitude ratio does not change enough to be easily discernible.

Figure 25 gives the relative amplitude of diffracted waves behind a spherical obstacle. The diameters of the magma chambers in the Katmai volcanic region are in general comparable to or smaller than the wavelengths corresponding to the frequency ranges for which the shadow boundary is sharp, therefore making the use of short-period high-frequency response instruments critical in such work.

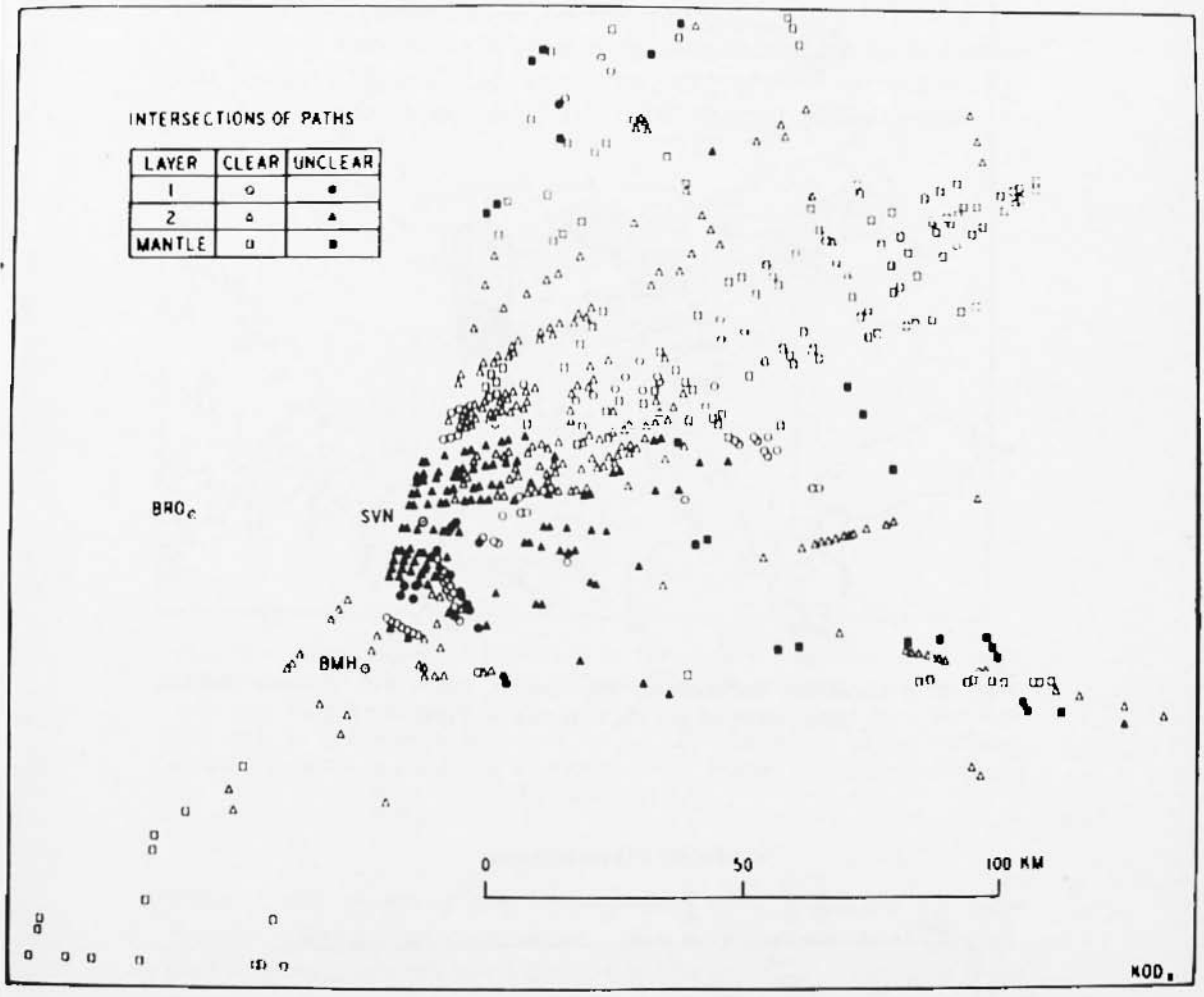

Fig. 22. – Map of path intersections for the *S*-waves. See legend. North is vertical. Seismic station abbreviations are: BHM, Baked Mountain; BRO, Brooks; KOD, Kodiak; SVN, Savonoski [from Kubota and Berg ([21])].

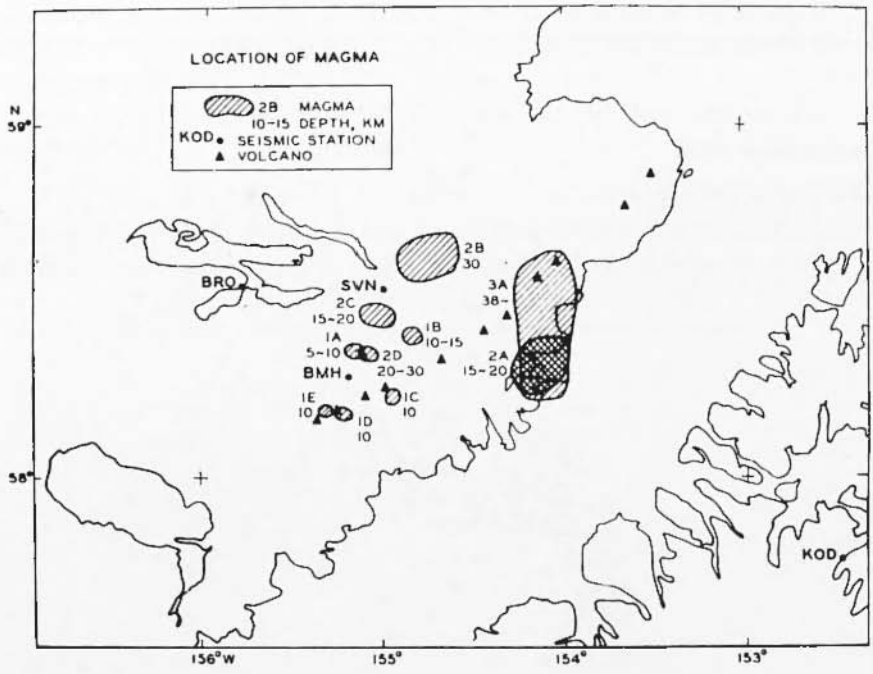

Fig. 23. – Locations deduced for the magma reservoirs. Seismic station abbreviations are the same as in Figure 22 ([21]).

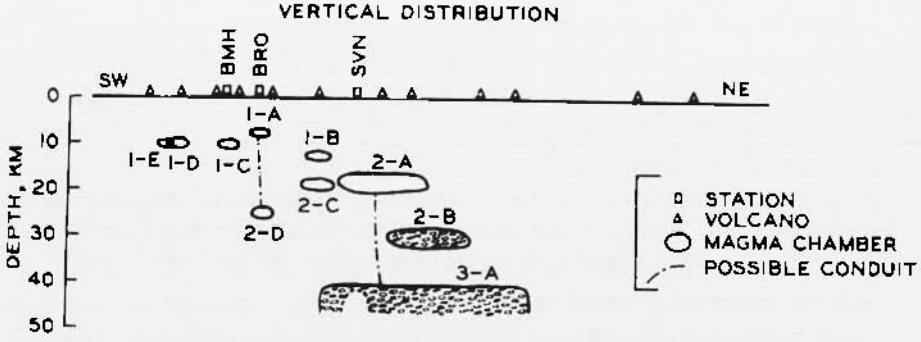

Fig. 24. – Cross section of the magma chambers northwest of Shelikof Strait, projected onto a common vertical plane. See legend. Seismic station abbreviations are the same as in Figure 22 ([21]).

(2) Accuracy of the ray-path plottings; which in turn rests on the accuracy of the focal determination and on the availability of a good crustal structure model for the region.

Further work in the Katmai region was carried out by Matumoto and Ward [23] following the installation of three stations, each consisting of a tripartite array of HS-10 (2 cps) vertical geophones and am-

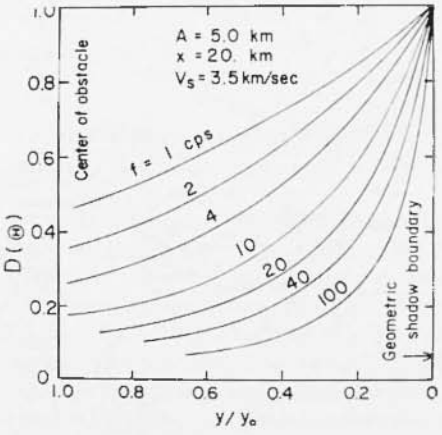

Fig. 25. – Distribution of amplitude in the shadow region of an obstacle, as a function of frequency. The distance from the geometric shadow boundary (the high-frequency limit) is denoted by y; the distance from the shadow axis to the shadow boundary by y_0. The frequency of the incident continuous wave is f and the amplitude is the Fresnel integral, $D(\Theta)$ [from Matumoto [22]].

plifiers. The recording was accomplished by a 7-channel FM tape recorder operated at slow speed. The response of the high-gain, high-frequency system was 10^7 at $\sim$ 80 Hz and $\sim 7 \cdot 10^5$ at $\sim$ 5 Hz decreasing linearly in the range with a 6 db slope and with a 12 db slope for lower frequencies. The locations of the stations are given in Figure 26. Detection of magma chambers in the Katmai area was reported by Matumoto [22] after analysis of records from this network showed S-wave screening and attenuation of the higher frequencies of P waves. The seismic activity was found to be concentrated in zones of active volcanism and most of the epicenters to be at shallow depth, usually less than 10 km. The disappearance of shear waves, attributed to a shadow effect by magma chambers, is controlled by the diffraction of

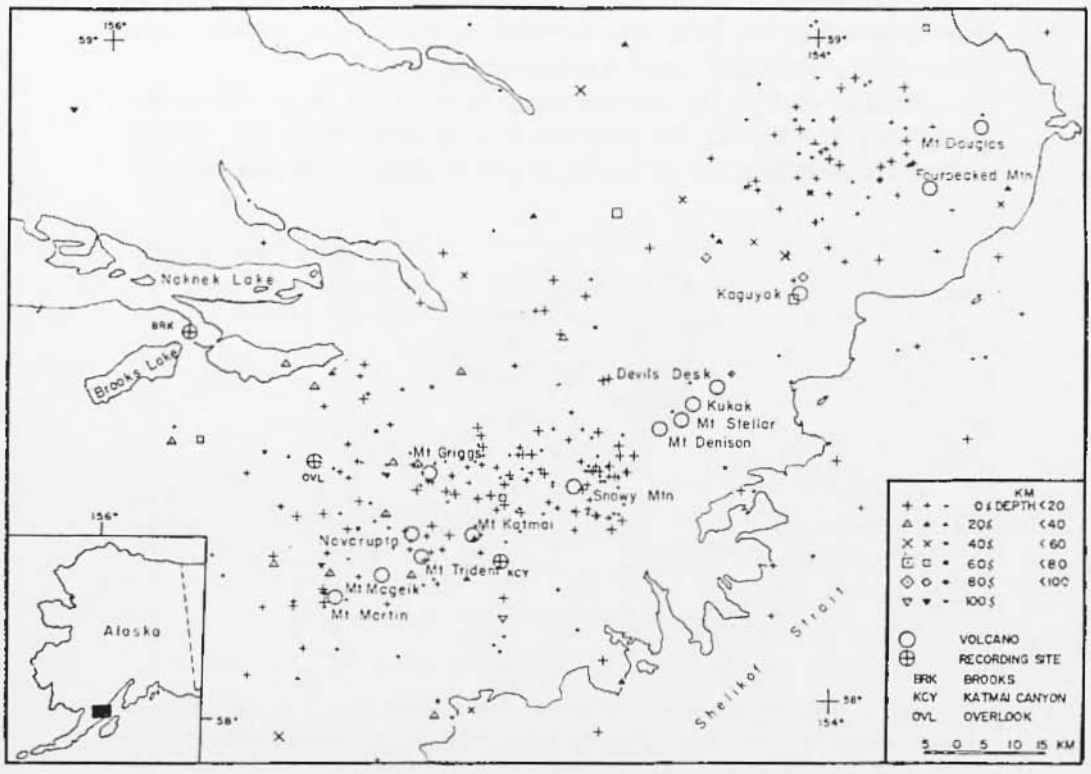

Fig. 26. – Map of Katmai National Monument in Alaska showing the location of the recording sites, the volcanoes, and the microearthquake epicenters for summer 1965. See legend; the larger the symbol, the more precise the hypocentral determination, based on the time resolution of the first arrivals and the clarity of the S waves [from Matumoto and Ward ([23])].

elastic waves, the geometry of the situation being strongly dependent on the shape of the obstacle. Theoretical studies by Teng and Richards ([29]) and by Phinney and Cathers ([25]) show that, for a hollow cylinder with a horizontally oriented axis, as the wavelength of an incident wave increases, the zone in which the amplitude of a wave becomes half that of the incident wave becomes larger. Also, the shadow zone is larger for incident P and SV waves and smaller for incident SH waves, as seen in Figure 27. The theory therefore points out that the difference in amplitude of SV and SH waves can be accounted for without having to assume a flat spheroidal shape for the chambers,

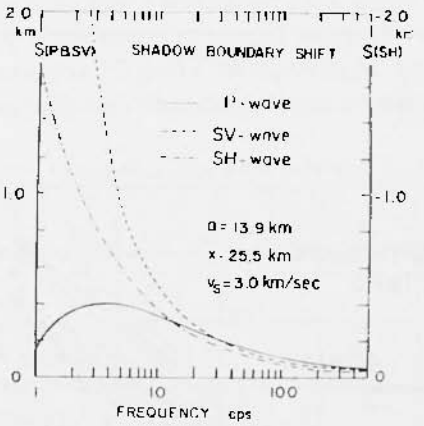

Fig. 27. – Dependence on frequency of the effective shadow boundary shift for waves diffracted from an hollow cylinder. Calculated for three types of waves (see legend) for specific values of the cylinder radius, a; the distance behind the obstacle of the observation point, x; and the shear-wave velocity, V_s. Note that there is significant shift for the shadow boundary only for the SV and SH waves at relatively low frequencies. The SV waves have a positive shift of the shadow boundary, hence an enlargement of the shadow zone, but the SH waves, which use the right-hand scale, have a negative, inward shift of the shadow boundary, actually a decrease of the shadow zone. The shift in the shadow boundary of P wave is not significant for the range of frequencies shown. [From Matumoto, 1971, as modified after Teng and Richards ([29])].

as did Kubota and Berg ([21]). For events from specific areas, high-frequency (10 to 20 cps) P waves are strongly attenuated when the S-wave is screened off. Using a crustal model of Matumoto and Page ([24]) the ray paths for the best-located events were plotted and are shown in Figure 28. The differences in travel time to the elements of an array provide azimuths of wave paths and apparent velocities; for a horizontally layered medium, using

$$v_a = v_i / \cos \delta_i$$

$$h = \sum_{i=1} D_i \tan \delta_i = \sum_{i=1} D_i \sqrt{(v_a^2 - v_i^2)/v_i}$$

where v_i = wave velocity in layer i

δ_i = angle of emergency of wave in layer i

D_i = distance,

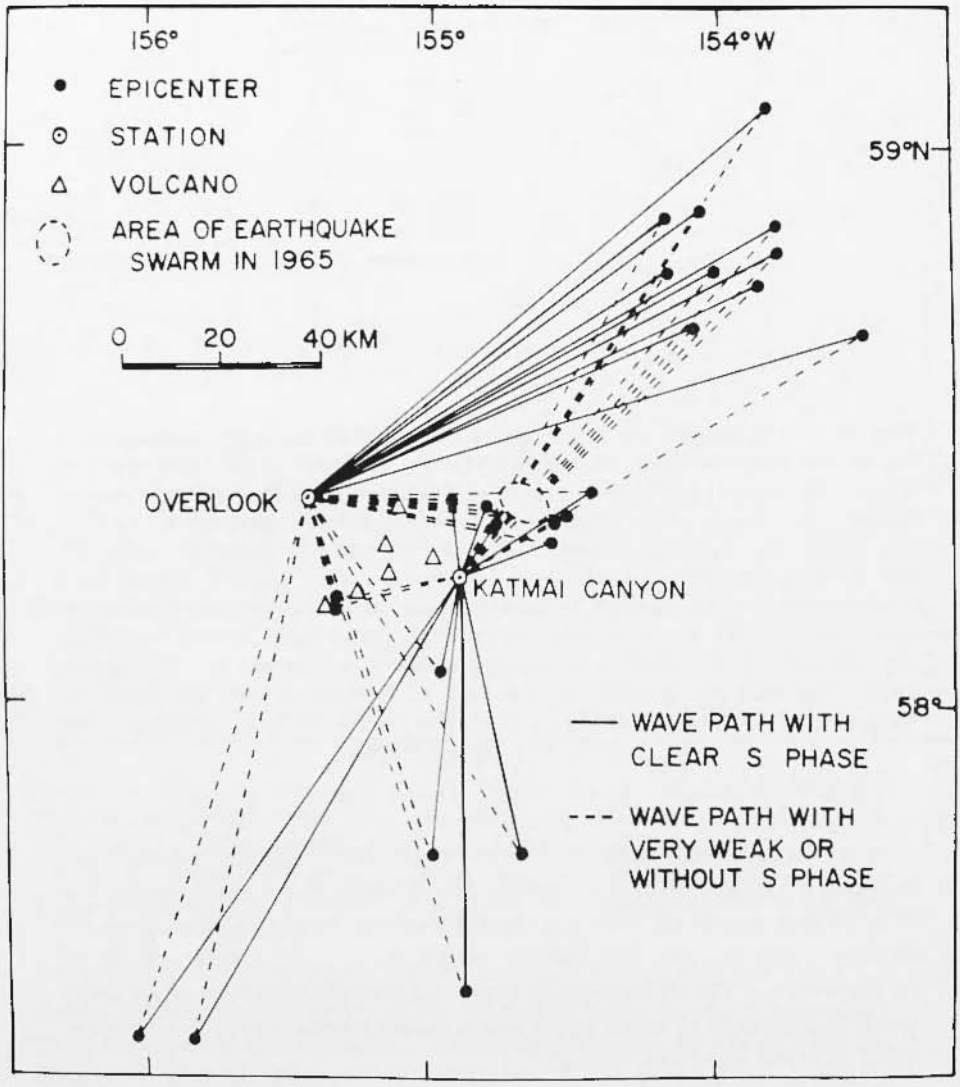

Fig. 28. – Map of the Katmai Peninsula, Alaska, showing the epicenters of earthquakes having ray paths with a distinct contrast in S-wave amplitudes. Triangles denote the active volcanoes. The epicentral area of an earthquake swarm recorded in 1965, is shown northeast of the Katmai Canyon seismic station, encircled by a broken line. [Modified from Matumoto ([22])].

the depth h can be uniquely determined at a given distance D for a crustal model with increasing downward velocity, so that a plot of azimuth versus apparent velocity is equivalent to one of azimuth versus depth. A comparison of such plots for events with and without

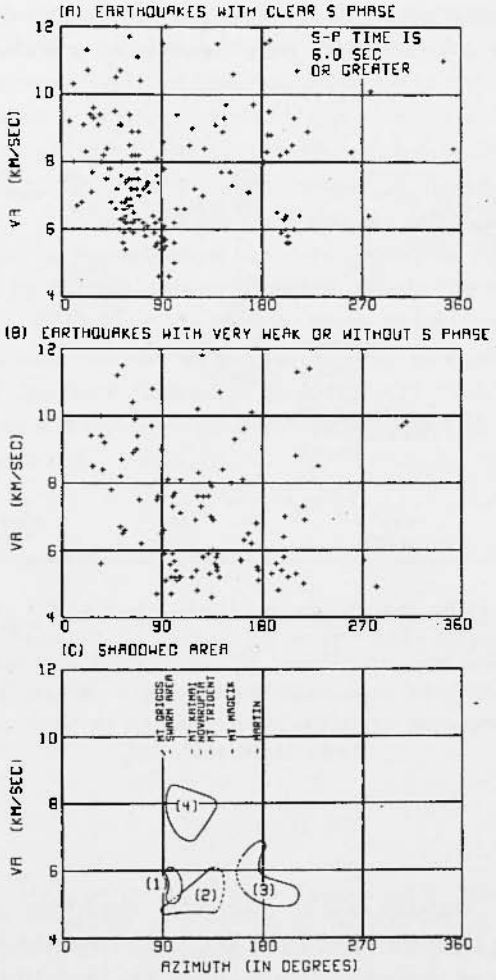

Fig. 29. – Three figures showing data on graphs of apparent velocity (VA) at Overlook Hill seismic station (see Figure 28 for location) versus azimuth. (A) shows those events having a clear S phase; (B) those with a very weak or not identifiable S phase. The difference in the spatial distribution of the events in (A) and (B) is considered significant. (C) shows specific domains in which distinctive differences in the distribution are observed [from Matumoto ([22])].

S waves allows delineation of zones of melting, i.e., magma chambers, as shown in Figure 29. The key factor in the precision with which those zones can be determined is the number of events along the marginal areas and the accuracy in array measurements, which in turn depends on its size, details of the crustal structure available, and precision of phase readings. Four chambers, three shallow (less than 10 km) and one deeper (20 to 30 km) were located and are shown in the map of Figure 30.

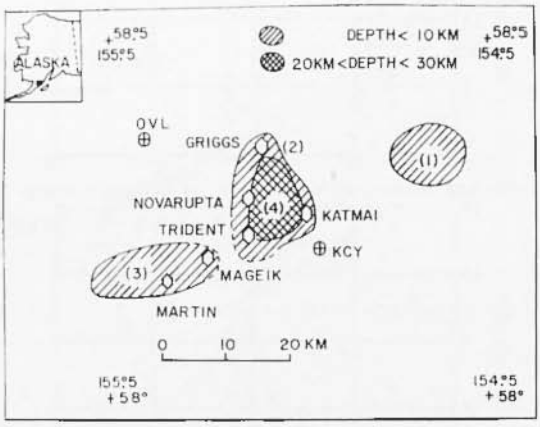

Fig. 30. Map of Katmai Peninsula, Alaska, showing the surface projection of the loci of magma chambers as determined by the shadow effect on the *S* wave. Three of them (1, 2, and 3) are at shallow depth, probably less than 10 km; and one (4) is probably between 20 to 30 km. Depths are determined by the apparent velocities corresponding to those in Figure 29 (C). [from Matumoto ([22])].

Discussion

From the Russian work, magmatic chambers are inferred at depths ranging between 35 and 110 km, while from the work at Katmai they are found at shallower depths, from less than 10 to 35 km. The study of the Katmai region was carried out on the basis of the complete screening of the *S* waves, while that of Kamchatka was based on the anomalous amplitudes of both *P* and *S* waves. Disappearance of *S* waves was not observed in Kamchatka, possibly because of the requirement that for a shadow zone to be effective the dimensions of the magma chambers must be comparable to or larger than the wavelengths;

or, alternatively, because attenuation is more effective at high frequencies; or, possibly because of the difference in magma viscosities in the two areas.

It is also interesting to note from these two cases how the range of depth of the magmatic chambers differs, raising the question, if both studies are correct in their results, of the possibility of the existence under a single volcanic edifice of deep chambers feeding more superficial ones, or alternatively, of their permanence in time. Further work in this field seems required in view of the possibility of finding an answer to this type of question that is directly related to the mechanism of volcanism, and also because determination of magma chamber locations — so far unattempted for the great majority of the world's volcanoes — could be important in the development of programs aimed at obtaining the geothermal power needed to satisfy the world's increasing energy needs. With regard to the last point, the delineation of magma-filled cavities could be extremely useful since new techniques for the extraction of geothermal energy from hot dry rock have now been proposed ([26]) and theoretical analyses that support the new techniques have been made ([15]).

ACKNOWLEDGEMENTS

The authors are beholden to Dr. Gordon A. Macdonald for reading the manuscript and to Mrs. Ethel McAfee for editing the manuscript. The authors remain solely responsible for the opinions expressed, however.

REFERENCES

([1]) ADAMS, W. M. MANSFIELD, 1964. – *Estimating the Spacial Dependence of the Transfer Function of a Continuum*, "Hawaii Institute of Geophysics", Rept. HIG 64-22, University of Hawaii, 13 pages.

([2]) ADAMS, W. M., and FURUMOTO A. S., 1965. – *A seismic refraction study of the Koolau volcanic plug*. "Pacific Sci.", 19 (3), 296-305.

([3]) BALESTA, S. T., and FARBEROV A. I., 1968. – *Seismic studies of Piip crater break-through*. "Bull. Volcan.", **XXXII**, 395-399.

([4]) BERG, E., KUBOTA S., and KIENLE J., 1967. – *Preliminary determination of crustal structure in the Katmai National Monument, Alaska*. "Bull. Seis. Soc. of America", **57**, 1367-1392.

(5) Eaton, J. P., and Murata K. J., 1960. – *How volcanoes grow*. "Science", **132**, 925-938.

(6) Farberov, A. I., and Gorelchik V. I., 1971. – *Anomalous seismic effect under volcanoes and some features of deep seated structure of volcanic areas*. "Bull. Volcan.", **XXXV**, 212-224.

(7) Fedotov, S. A., 1973. – *Deep Structure under the Volcanic Belt of Kamchatka, in "The Western Pacific: Island Arcs, Regional Seas, Geochemistry"*. Univ. W. Aust. Press, Nedlands, W. Australia, P. J. Coleman editor.

(8) Fedotov, S. A., and Farberov A. I., 1966. – *On screening of shear seismic waves and on magmatic chamber in the upper mantle under Avacha Volcano region*. Coll. "Volcanism and deep structure of the Earth", Publ. "Nauka", 43-48 (in Russian).

(9) Firstov, P. P., and Shirokov V. A., 1971. – *Seismic investigation of the roots of the Kliuchevskaya group volcanoes, Kamchatka*. "Bull. Volcan.", **XXXV**, 164-172.

(10) Furumoto, A. S., Thompson N. J., and Woollard G. P., 1965. – *The structure of the Koolau Volcano, from seismic refraction studies*, "Pacific Sci.", **19** (3), 306-314.

(11) Furumoto, A. S., and Adams W. M., 1968. – *Seismic refraction study of the internal structure of a volcanic cinder cone, in Geophys. Mon. 12. The crust and upper mantle of the Pacific area*. "A. G. U", Washington, D. C., 112-121.

(12) Gardner, L. W., 1949. – *Seismograph determination of salt dome boundary using well detector deep on dome flank*. "Geophysics", **14** (1), 29-38.

(13) Gorshkov, G. S., 1956. – *On the depth of magmatic chamber of Kliuchevskiy Volcano*. C. R. (Doclady) "Ac. Sc. USSR", **106**, 4, 703-705 (in Russian).

(14) Gorshkov, G. S., 1971. – *Prediction of Volcanic Eruptions and seismic methods of location of magma chambers. A review*. "Bull. Volcan.", **XXXV**, 198-211.

(15) Harlow, F. H., and Pracht W. E., 1972. – *A theoretical study of Geothermal energy extraction*. "J. Geophys. Res.", **77**, 7038-7048.

(16) Hayakawa, M., et al. – *Seismic Surveys on Showa Shinzan, 1955*. Paper presented at 15th meeting of the Seismological Society of Japan, May 9.

(17) Hill, D. P., 1969. – *Crustal structure of the island of Hawaii from seismic refraction measurements*. "Seis. Soc. of Am. Bull.", **59** (1), 101-130.

(18) Jackson, E. D., 1968. – *The character of the lower crust and upper mantle beneath the Hawaiian Islands*. 23rd International Geolog. Cong., Prague, Czechoslovakia.

(19) Kienle, J., 1970. – *Gravity traverses in the valley of Ten Thousand Smokes, Katmai National Monument, Alaska*, "J. Geophys. Res.", **75**, 6641-6649.

([20]) KINOSHITA, W. T., KRIVOY H. L., MABEY D. R., and MACDONALD R. R., 1963. – *Gravity survey of the island of Hawaii.* U. S. Geol. Surv. Prof. Paper, 475-C, 114-116.

([21]) KUBOTA, S. and BERG E., 1967. – *Evidence for Magma in the Katmai volcanic range.* "Bull. Volcan.", **XXXI**, 175-214.

([22]) MATUMOTO, T., 1971. – *Seismic body waves observed in the vicinity of Mount Katmai, Alaska, and evidence for the existence of molten chambers".* "Bull. Geol. Soc. Am.", **82**, 2905-2920.

([23]) MATUMOTO, T., and WARD P. L., 1967. – *Microearthquake study of Mount Katmai and vicinity, Alaska.* "J. G. R.", **72**, 2557-2568.

([24]) MATUMOTO, T., and PAGE R., 1969. – *Microaftershocks following the Alaska earthquake of March 28, 1964; Determination of hypocenters and crustal velocities in the Kenai Peninsula-Prince William Sound area, in the Prince William Sound, Alaska earthquake of 1964 and aftershocks.* "U. S. Coast and Geod. Survey", Pub. 10-3, pt. B, 157-174.

([25]) PHINNEY, R. A., and CATHERS L. M., 1969. – *Diffraction of P by the core; a study of long period amplitudes near the edge of the shadow.* "J. G. R.", **74**, 1556-1574.

([26]) ROBINSON, E. S., POTTER R. M., MCINTEER B. B., ROWLEY J. C., ARMSTRONG D. E., MILLS R. L., and SMITH M. C., 1971. – *A preliminary study of the nuclear subterrene.* Report No. LA-4547, Los Alamos Scientific Laboratory, Los Alamos, N. M.

([27]) RYALL, A., and BENNETT D. L., 1968. – *Crustal structure of southern Hawaii related to volcanic processes in the upper mantle.* "J. G. R.", **73**, 4561-4582.

([28]) SBAR, M. L., and MATUMOTO T., 1971. – *Refraction profiles in the Valley of Ten Thousand Smokes, Katmai, Alaska.* "Bull. Volcan.", **XXXV**, 335-349.

([29]) TENG, T. L., and RICHARDS P. G., 1969. – *Diffracted P, SV, and SH waves and their shadow-boundary shifts.* "J. G. R.", **74**, 1537-1555.

([30]) WARD, P. L., and MATUMOTO T., 1967. – *A summary of volcanic and seismic activity in Katmai National Monument, Alaska.* "Bull. Volcan.", **XXXI**, 107-129.

([31]) WILLIAMS, H., and MCBIRNEY A. R., 1968. – *An investigation of volcanic depressions. pt. 1, Geologic and geographic features of Calderas.* "NASA", Progress Report NGR-38-033-012, p. 1-87.

([32]) YOSHIKAWA, M., KAMO K., and KITSUNEZAKI C., 1959. – *Seismic exploration in the vicinity of the crater of Nakadate, Aso volcano.* "Bull. Volcan. Soc. Japan", **II**, 4 (1), 20-32.